Phys. Status Solidi RRL 3, No. 2–3, 70–72 (2009) / DOI 10.1002/pssr.200802264

pss +++rapid research letters+++
www.pss-rapid.com

Correlation of pre-breakdown sites and bulk defects in multicrystalline silicon solar cells

Dominik Lausch[*,1,2], **Kai Petter**[1], **Holger von Wenckstern**[2], **and Marius Grundmann**[2]

[1] Q-Cells SE, Process Development – Silicon Materials, OT Thalheim, Guardianstraße 16, 06766 Bitterfeld–Wolfen, Germany
[2] Universität Leipzig, Institut für Experimentelle Physik II, Linnéstr. 5, 04103 Leipzig, Germany

Received 10 December 2008, revised 22 January 2009, accepted 22 January 2009
Published online 30 January 2009

PACS 61.72.Lk, 61.72.Mm, 68.37.–d, 68.55.jm, 78.60.Fi

[*] Corresponding author: e-mail d.lausch@q-cells.com, Phone: +49-163-3344566

Strong correlation between the pre-breakdown sites visible in dark lock-in thermography due to local heating and the intensity of spatially resolved electroluminescence of reverse-biased solar cells was observed. By comparing differently texturised solar cells we could show that the pre-breakdown sites are not correlated to the surface morphology, e.g. etch pits resulting in local field enhancement. The positions of the pre-breakdown sites are identical for acidic and alkaline texturised solar cells and therefore are directly related to bulk defects in the wafer. Nevertheless, the breakdown voltage is lower for acidic texturised solar cells; the parameters of breakdown are influenced by the texture in contrast to the position. Also pre-breakdown sites are observed in areas without specific surface features for alkaline texturised solar cells.

1 Introduction Light emission associated with electrical breakdown from reverse-biased p–n junctions has been reported for various materials such as Si [1], Ge [2], GaAs [3] and ZnSe [4]. Broad luminescence spectra with transition energies higher and lower than the band gap were found. Different models describe this light emission as a result of interband recombination [1, 5], intraband transition within the conduction or valence bands [5] or bremsstrahlung of hot carriers in the Coulomb field of charged centres [6].

In solar cells the breakdown occurs at lower voltages than it would be expected for parallel plane junctions. Pre-breakdown is an important phenomenon in partially shadowed photovoltaic modules. Shadowing of individual solar cells in a module leads to reverse biasing of the shadowed cells [7]. The reason for this local and early breakdown is unclear. Bauer et al. [8] suggested that the pre-breakdown occurs because of an enhancement of the electric field at etch pits, introduced in vicinity of defects by the acidic texture. Such field enhancement is described by Baliga et al. [9]. Recently, Kwapil et al. demonstrated that pre-breakdown of acidic texturised solar cells can be divided into three stages [10]. Two of these stages are connected to edge effects (stage I) or regions with short carrier lifetime (stage II); both have a voltage dependence characteristic of a soft breakdown and dissipate only little heat. However, most heat is generated at sites showing a hard breakdown at about –12.5 V (stage III) located in regions with long carrier lifetime. Nevertheless, the origins of the pre-breakdown as well as the current transport mechanism are still under debate.

In the following we will show by using previously unachieved high spatial, microscopic resolution of pre-breakdown sites that field enhancement at etch pits is not the prime cause for pre-breakdown in our samples. A comparison of silicon solar cells fabricated with two industrially most prevalent surface preparation methods (acidic and alkaline) reveals that the position of the pre-breakdown sites is determined by the bulk defect structure of the wafers. However, not all bulk defects cause pre-breakdown sites.

2 Sample preparation The samples analyzed are silicon solar cells fabricated with a commercial process based on B-doped (acceptor concentration $N_A \approx 10^{16}$ cm^{-3}) 156×156 mm^2 multicrystalline silicon wafers. The samples were sorted into two batches of neighboring wafers (in

relation to the block from which they were cut). In particular the position of bulk defects such as grain boundaries and dislocations is similar as checked with optical microscopy after defect etching. Only slight differences caused by the 200 µm kerf loss during the sawing process and 200 µm wafer thickness can be expected. Both batches were processed identically except for the texturing. One batch was texturised with KOH (alkaline texture) and the other with a mixture of HF and HNO_3 (acidic texture). After etching with the anisotropic alkaline texture solution the surface morphology depends on the crystallographic orientation of the different grains; crystal defects are not delineated. The isotropic acidic etch creates a texture independent of the crystallographic orientation and acts as a defect etch such that etch pits caused by grain boundaries and dislocations are revealed. Such etch pits are clearly revealed in scanning electron microscopy images (not shown here).

3 Measurement tools Spectrally integrated, spatially resolved reverse-bias electroluminescence intensity images (ReBEL) were acquired at room temperature using a camera with a Si CCD. Magnified images (µ-ReBEL) were obtained using a Carl Zeiss microscope. In order to facilitate the comparison between sites of luminescence and surface structure, information of reflected-light microscopy is overlaid with the ReBEL images. The dark lock-in thermography (DLIT) measurements were recorded with an Aescusoft 2100 measurement device.

4 Results and discussion The dark current–voltage characteristics of the two cells investigated did not reveal ohmic shunts. The breakdown voltage of the acidic texturised cell is about –13 V and that of the alkaline texturised cell about –17 V. Both cases exhibit a hard breakdown. As mentioned in the introduction the high heat dissipation occurs for hard breakdowns (called stage III in Ref. [10]), all of the following ReBEL measurements were conducted at –13 V and –17 V for the acidic and alkaline texturised cell, respectively. The current is in each case about 460 mA.

Figure 1a shows a ReBEL image and Fig. 1b a DLIT measurement at room temperature. Bright spots of high

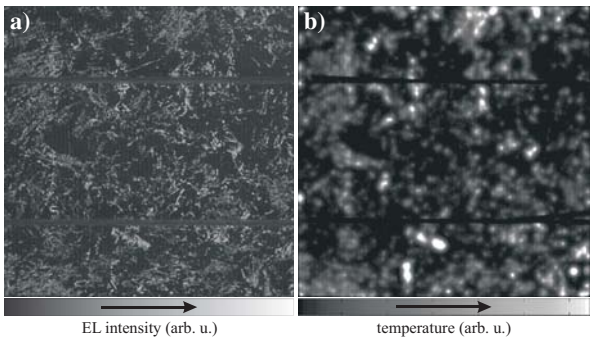

Figure 1 (a) Spectrally integrated, spatially resolved reverse-bias EL (ReBEL) and (b) dark lock-in thermography (DLIT) measurement of a 6″ acidic texturised reversed-biased solar cell ($U = -13$ V). Horizontal lines are due to front contact grid.

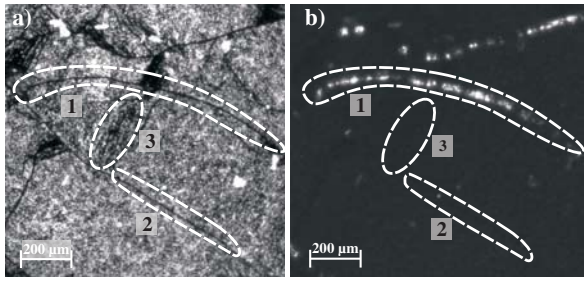

Figure 2 (a) Microscopic image and (b) microscopic EL image (µ-ReBEL) of an acidic texturised solar cell. Three prominent regions are marked. Regions 1 and 2 contain grain boundaries. Region 3 is an area with a high dislocation density.

EL intensity (Fig. 1a) are visible as pre-breakdown sites in the DLIT measurement (Fig. 1b). The pre-breakdown sites are exactly at the same positions as the spots of high EL intensity similar to recent results of Kwapil et al. [10]. An advantage of EL at reverse biased solar cells compared to the DLIT measurements is the much higher spatial resolution which makes it possible to resolve the pre-breakdown sites in more detail as discussed below.

Figure 2 shows a microscopic investigation of pre-breakdown sites. By the comparison of an image of the surface structure of an acidic texturised solar cell (Fig. 2a) and the microscopic EL image (Fig. 2b) of the same area, it is revealed that regions emitting light at reverse bias are located at etch pits related to crystal defects (in this case a grain boundary – region 1). Further, the luminescence is strongly localized indicating the formation of microplasmas due to local avalanche breakdown [11]. The grain boundary in region 2, however, does not give rise to any electroluminescence. Dislocations inside a grain (distant from a grain boundary) never showed luminescence in the investigated spectral range of about 400–1100 nm for all cells investigated (region 3). Note, this comparison is only possible for acidic texturised silicon solar cells since the alkaline texture will not reveal surface defects.

Figure 3 shows the spectrally integrated, spatially resolved EL images of reverse-biased acidic (Fig. 3a, c and e) and alkaline (Fig. 3b, d and f) texturised neighboring solar cells in three different magnifications (µ-ReBEL). Despite a different surface morphology due to the different texture the spots of high EL intensity are at the same positions.

The µ-ReBEL images in Fig. 3 with higher magnification clearly show that the positions of high EL intensity are located at grain boundaries and coincide almost perfectly for both texturisations. Even at 50× magnification (Fig. 3e and f) only minor differences of the positions of the EL sites can be observed. These small differences are attributed to the distance of the investigated positions in the ingot (200 µm wafer thickness + 200 µm kerf loss). The most prominent difference is the blurred luminescence in the acidic texturised solar cell (Fig. 3e) probably due to diffuse optical scattering by the surface texture.

From this comparison we conclude that the position of the pre-breakdown sites is not determined by the etch pits

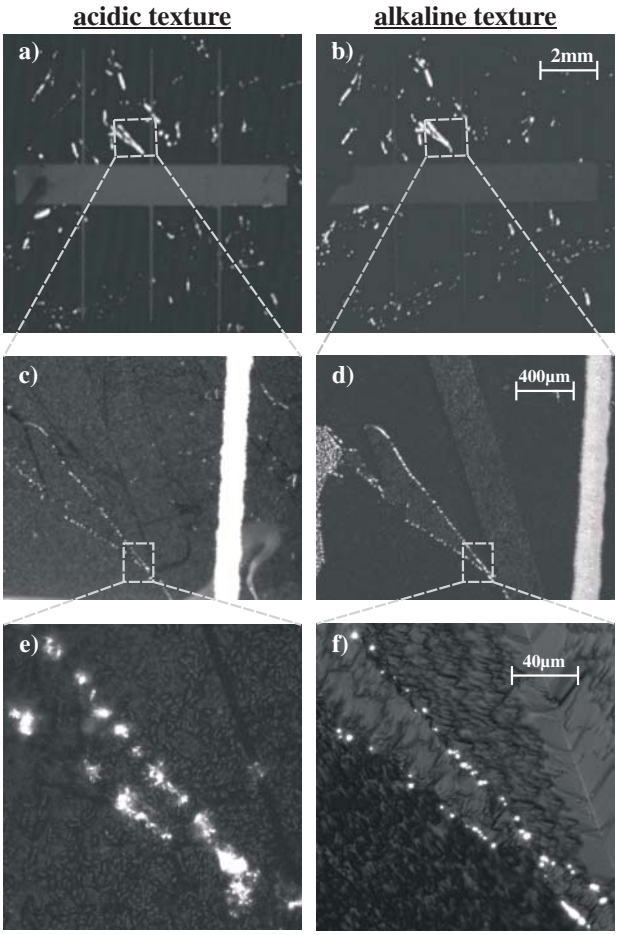

Figure 3 µ-ReBEL of an acidic (a, c, e) ($U = -13$ V) and an alkaline (b, d, f) ($U = -17$ V) texturised solar cell processed from a neighboring wafer for different magnifications. Areas in grey boxes are depicted with higher magnification below the respective picture.

introduced by the acidic texture. The fact that the pre-breakdown occurs at the same positions for both texturisations is clear evidence that pre-breakdowns are mainly caused by certain defects in the bulk of the wafer.

The example shown in Fig. 4 supports this conclusion. Figure 4b shows a microscopic image of a nearly flat surface region of an alkaline texturized cell. No field enhancement can be expected. However, we observed light emission at pre-breakdown sites shown in the microscopic EL image of Fig. 4d caused by bulk defects of the wafer. These defects in the bulk of this area of the wafer at these positions are clearly revealed in the neighbouring acidic texturised solar cell depicted in Fig. 4a and c. Also in these samples the surface morphology has no influence on the position of the pre-breakdown sites.

In summary our investigations show that the position of the pre-breakdown sites visible due to heat generation in DLIT can be correlated to sites emitting light in reverse biased solar cells. By comparing acidic and alkaline texturised solar cells we could show that proper surface preparation does not lead to pre-breakdown sites. Instead they are solely determined by the bulk (multicrystalline) structure itself. However, the voltages at which this pre-breakdown occurs are lower for acidic texturised cells than for alkaline texturised cells. Therefore, the field enhancement at etch pits for the acidic texturised cells influences the voltage at which the pre-breakdown occurs. The question that remains open is why a pre-breakdown and associated light emission is observed near certain grain boundaries while others seem to be inactive in this respect. In further investigations we will explore whether the pre-breakdown can be correlated to the electrical activity of the different defects.

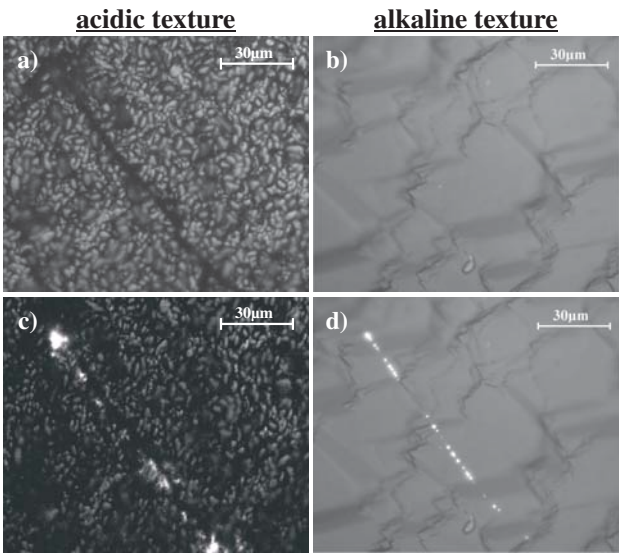

Figure 4 (a) Microscopic image and (c) microscopic EL image of an acidic texturised solar cell. (b) Microscopic image and (d) microscopic EL image of an alkaline texturised solar cell. The bulk defects at these positions are revealed only in the acidic texturised solar cell.

Acknowledgement We thank the lab team of Q-Cells SE for their diverse and valuable support.

References

[1] A. G. Chynoweth and K. G. McKay, Phys. Rev. **102**, 369 (1956).
[2] A. G. Chynoweth et al., Phys. Rev. **118**, 425 (1960).
[3] A. E. Michel et al., J. Appl. Phys. **35**, 3543 (1964).
[4] K. Turvey and J. Allen, J. Phys. C **6**, 2887 (1973).
[5] P. A. Wolff, Phys. Rev. **95**, 1415 (1954).
[6] T. Figielski and A. Torun, Int. Conf. Phys. Semiconductors, Exeter, 1962, p. 863.
[7] A. Woyte et al., Sol. Energy **74**, 217 (2003).
[8] J. Bauer et al., Phys. Status Solidi RRL **3**, 40 (2009).
[9] B. J. Baliga and S. K. Ghandhi, Solid State Electron. **19**, 739 (1976).
[10] W. Kwapil et al., Proc. 23rd European Photovoltaic Solar Energy Conference, Valencia, Spain, edited by D. Lincot, H. Ossenbrink, and P. Helm (WIP, Munich, 2008), p. 1797.
[11] S. Mahadevan et al., Phys. Status Solidi A **8**, 335 (1971).

